DOI: 10.1007/s12541-012-0177-1

Precise Detection and Elimination of Grid Injected DC from Single Phase Inverters

Ashraf Ahmed[1,#] and Ran Li[2]

1 School of Electrical Engineering, Soongsil University, 369 Sangdo-ro, Dongjak-gu, Seoul, Korea, 156-743
2 School of Engineering and Computing Sciences, Durham University, South Road, Durham, UK, DH1 3LE
Corresponding Author / E-mail: ahmed@ssu.ac.kr, TEL: +82-2-828-7098, FAX: +82-2-817-7961

KEYWORDS: Dc current injection, H-bridge inverter, Signal-noise ration, Closed-loop control, Measurement filter

Single-phase voltage source inverters are used for connecting small scale renewable energy sources to low voltage distribution networks. They operate to supply the network with sinusoidal current. If output transformers are not used, these inverters must prevent excessive dc current injection, which may cause detrimental effects in the network. In this study, the causes of dc current injection in a common inverter topology are analyzed. This work explains the design and test of a passive filter circuit precisely measuring the dc component in the inverter output current. The filtered dc signal is then used to control the single phase inverter for the objective to keep the dc injection low – below the standard limit. Characteristics of the proposed method are illustrated using simulation and experimental results.

Manuscript received: January 11, 2012 / Accepted: March 7, 2012

NOMENCLATURE

C_{res} = Filter resonance capacitance (F)
G_m = Transfer function of the measurement circuit
i_{main} = Main output current of the inverter (A)
$I_{main\text{-}dc}$ = Dc component in i_{main} (A)
i_b = Current through the Filter blocking inductance (A)
v_{inv} = Ac output voltage at the inverter terminals (V)
v_m = Measured voltage signal through resistance R_m (V)
$V_{m\text{-}dc}$ = Dc component in v_m (V)
m_a = Inverter modulation index
L_f = Main inverter filter inductance (H)
L_b = Inductance to block the ac component of i_{main} (H)
L_{res} = Filter resonance inductance (H)
L_m = Inductance to block ac component form v_m (H)
R_m = Measuring signal resistance (Ω)
R_a = Main current measuring resistance (Ω)

1. Introduction

As the market for small scale distributed renewable energy generation systems is rapidly increasing the need for power electronic converters increases.[1,2] The inverter is necessary in the system to produce a sinusoidal wave which could be supplied to the ac load or to the grid.[3] The single phase H-bridge inverter is a simple circuit topology with a small number of components. Furthermore, it is simple to control with one disadvantage which is represented in the dc injection problem.

This study is concerned with the risk of dc injection into the network from the small scale single-phase inverters without output transformers. Due to the approximately short circuit characteristic of the ac network, a little dc voltage component that can accidently be produced by the inverter will produce large dc injection. This causes detrimental effects on the network components, particularly the network transformers which can saturate, resulting in irritant tripping. This may also increase the losses in and reduce the lifetime of the transformers, if not tripped. Moreover, the existence of the dc component can induce metering errors and malfunction of protection relay.[4]

As the proposed system in this work is connected to the utility grid, it has to fulfill the quality standards for the dc component injected into the grid value. The IEEE-929 standard permits a limit of 0.5% of the rated output current. However, the European IEC61727 suggests dc injection limits less than 1%. Other standards in the world have fewer restrictions and are easier to cope with.[5-11] In this study, the work will focus to fulfill these standards. This paper presents a method of complying with such a requirement by an inverter that does not have a network side output

transformer.

The inclusion of a low frequency (50 or 60 Hz) isolation transformer at the output of the inverter eliminates the injection of dc on the grid side. Drawbacks of using this type of transformer are cost, weight, and size added to the inverter system, as well as the reduced overall efficiency. A low frequency transformer is more bulky than a high frequency isolation transformer which however cannot prevent dc injection into the grid.[12,13]

For a transformerless topology, the research to overcome the dc injection problem could be basically classified into three categories; using other topologies, modifying the H-bridge topology and dc elimination using measurement circuits.

Using other topologies as half bridge inverter has been proposed to remove the dc injection to the grid. However, this causes many problems, such as using double dc link voltage, increased losses, and high size of the dc link capacitors. This also increases the overall cost and size of the inverter. Using such a kind of inverter will also increase the ripple and reduce the total harmonic distortion.[7,8] Another topology is neutral point diode clamped, which is proposed in this reference.[9,13] This topology has better efficiency compared to the basic half bridge inverter, but it still needs double the dc voltage value of the H-bridge, and bigger capacitors.

In the second category, the basic idea is to modify the H-bridge inverter to eliminate the dc component of the current. One of the topologies is to add switches in the dc side to clamp the voltage during the zero voltage periods.[14] This method could be also applied by clamping in the ac side.[15] Both methods could not guarantee elimination of dc component as the unbalance due to forward IGBTs voltages and PWM control would not be removed.

The third solution to the dc injection problem is to use a feedback control loop to eliminate the dc offset in the inverter output voltage and a similar approach is adopted in this study. Although this was also adopted in previous studies,[11,12,16] a challenge remaining to be addressed further is the accurate measurement of the usually very small dc component mixed by a large ac current fundamental value. Reference[9] proposes a method of auto-calibrating the current sensing device to remove its error. The dc component on the ac output side of the inverter is deduced from the reading of the calibrated current sensor on the dc side, assuming the knowledge of the inverter switching pattern. This method can reduce the dc injection but will not eliminate it, because it only intends to compensate the dc injection due to inaccuracy in the PWM process while the dc component caused by unequal on-state voltage of the semiconductor devices in the inverter cannot be compensated. Furthermore, the method is subject to the influence of noises and achieves its objective at the cost of increased inductance between the dc link capacitor bank and the inverter bridge which should ideally be kept as low as possible to constrain switching transient and avoid EMC problems.

The study focuses on a full bridge voltage source inverter operating in a unipolar PWM mode. The block diagram of the transformerless inverter under study is depicted in Fig. 1 showing the control for dc injection compensation.

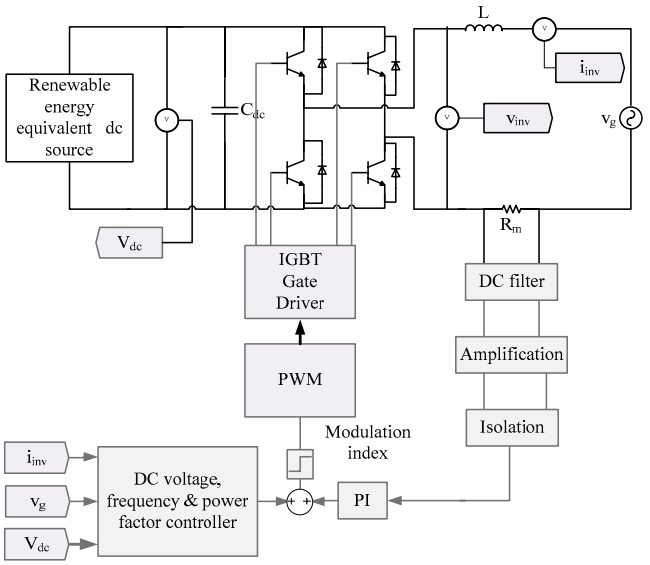

Fig. 1 The grid-connected inverter circuit and control

2. Causes of dc Injection

There are three main factors which can cause dc injection into the network from a single-phase H-bridge voltage source inverter. These are unequal semiconductor device characteristics in the inverter including on-state resistance and on-state forward saturation voltage, and the temperature coefficients of these parameters. The device characteristics are affected by inevitable variations during fabrication and packaging and can also drift in operation due to degradation mechanisms such as bond wire lift-off.

The circuit in Fig. 1 was built in Matlab/Simulink with Plecs software, and the simulation was performed assuming that the on-state voltage of the IGBT devices in the inverter is unbalanced by 0.05 V. Figure 2 shows the unbalance produced by the on state forward voltages at the output of the inverter (v_{inv}), see Fig. 1. A part of the positive cycle shows that the forward voltages in this leg of the inverter are the same. In the negative half cycle, one of the IGBTs has less forward voltage by 0.05 V. For a typical 230 V single-phase feeder, the series resistance in the thevenin equivalent circuit representation would be 0.01 Ω to 0.04 Ω. For a modulation index of 0.8 in the inverter and 1 kW output power at unity power factor, the simulation showed that the dc injection was between 375 mA and 1500 mA. This shows how difficult it is to comply with the typical standard requirements. The only way is probably to set the dc under close-loop control if a low frequency output transformer is to be avoided, which however depends on how accurately the weak signal of a small dc can be measured.

Dc bias that can be included in the inverter PWM switching process. This is particularly vulnerable to the blanking time between the upper and lower switches in the same leg of the bridge. Simulation shows that the dc injection in the range of hundreds of mA can be easily reached with unbalance of blanking time in a few microseconds between the positive and negative half cycles of the inverter output.

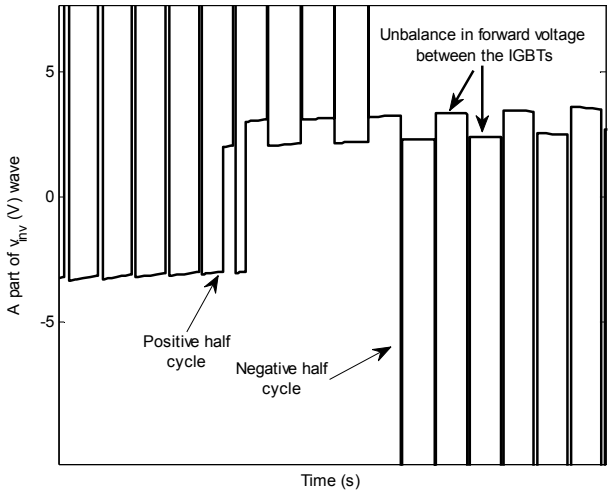

Fig. 2 Effect of unbalance in forward IGBT voltages

Dc bias of output current sensor, which also could provide dc bias to the PWM process. This will cause unbalance between the positive and negative half-cycles and causes dc component to be injected.

3. Topology and Measurement Circuit

Following the approach of active control as described in reference,[11] this study proposes a method of measuring the dc component in the inverter output current. The output current is measured by a resistive shunt and the obtained voltage signal processed by a specially designed and tuned analogue filter to increase the signal-noise ratio so that the dc level as specified in standards becomes measurable.[17] The response should be adequately fast even for renewable energy systems which are normally working under variable conditions. In the approach which is further pursued in this study, the dc component in the output current is sensed and used in the controller to eliminate the dc injection. One of the challenges to this approach is the accuracy, and this is due to the relatively small amount of dc component which needs to be accurately measured. As an illustration of this problem; the required specification many countries is 5 mA, which is less than 0.1% of the fundamental component. This is not easily measurable due to the offset and accuracy in the current measurement device. Another problem is the resolution as a very high DSP resolution is needed to measure the current directly from the line and to analyze it to find the dc component by filtering or FFT analysis. This will add cost to the inverter.

A circuit based on the resonance approach is proposed in this paper for measuring the dc component in the current. The circuit is shown in Fig. 3 as resistor R_a is the resistive current shunt in the path of the inverter output current. The series L_{res}-C_{res} resonance circuit is used to bypass the majority of the fundamental ac component measured across the shunt and block the dc component. As a result, the entire dc component of the shunt resistor voltage will be applied across the resistor R_m as C_{res} is blocking the dc component. L_b is used to block the main inverter current ac

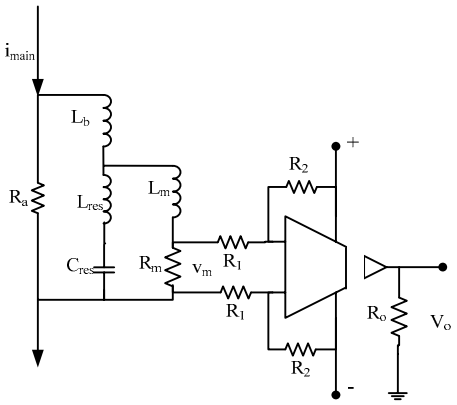

Fig. 3 The proposed dc component measurement circuit

component while L_m is used to force the ac signal to circulate through L_{res}-C_{res} branch. L_b and L_m are very important to block most of the ac signal increasing dc component ratio in the output signal v_m.

v_m is measured as an indication of the dc component contained in the inverter output current. v_m will contain a residual of the 50 Hz (or 60 Hz) ac component that has not been filtered out in spite of the last discussion. Nevertheless, for the reason to become clear later, this has little effect as long as much of the ac component has been bypassed and the signal-noise ratio regarding the targeted dc component in the measured current shunt voltage is significantly improved. A low offset differential amplifier is used to amplify the signal while another amplifier with isolated output is used to guarantee isolation between power and control circuits. Figure 3 shows only one amplifier for simplicity.

Analyzing the circuit in Fig. 3, the transfer function from the mains current (i_{main}) to the filter output voltage (v_m) in Laplace form can be deduced as in Equation (1).

$$G_m(s) = \frac{R_m R_a\left(sL_{res}+\frac{1}{sC_{res}}\right)}{\left(\left(R_a+sL_b\right)\left(R_m+s\left(L_m+L_{res}\right)+\frac{1}{sC_{res}}\right)+\left(sL_{res}+\frac{1}{sC_{res}}\right)\left(R_m+sL_m\right)\right)} \quad (1)$$

4. Choosing Measuring Circuit components

In this section, design of the values of the filter component will be proposed. There are three components need to be chosen, which are L_b, L_m, and R_m, and the resonance circuit filters. These components can be designed as follows:

The value of the inductance L_b is chosen according to the filter rating where L_b blocks the mains ac current component which is a short circuit to the dc component. L_b can be chosen according to

$$L_b = \frac{R_a}{\omega}\frac{i_{main}}{i_b} \quad (2)$$

Where (ω) is the mains frequency (rad/s), i_b is the ac current through L_b and i_{main} is the inverter output rated current.

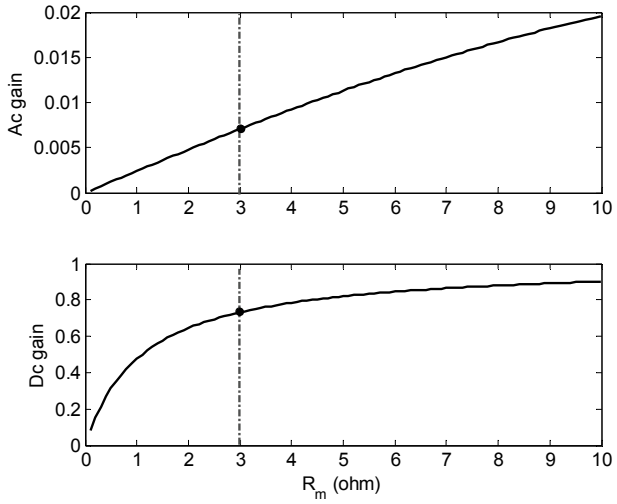

Fig. 4 Choosing filter output resistance R_m

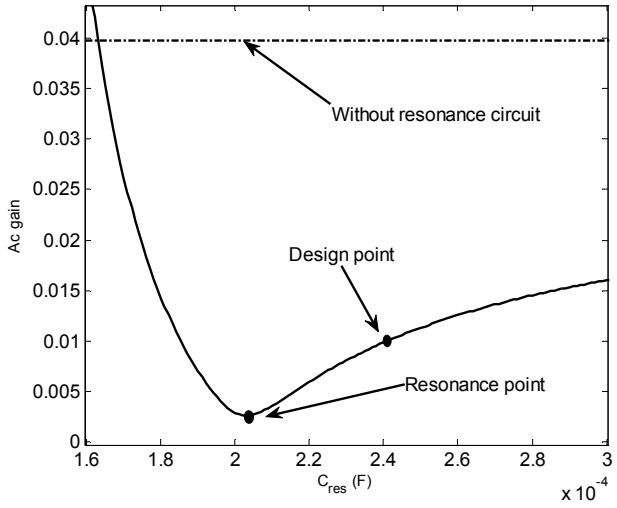

Fig. 5 Choosing resonance filter components

The value of inductance L_m is chosen to give some tolerance in L_{res} and C_{res} in the series resonant branch.

To choose the precise value for the resistance R_m, the steady state transfer functions are considered from the dc or the fundamental ac component in the inverter output current to the corresponding components in v_m. The ac gain is calculated by giving $s = \omega$ in Equation (1) as $\omega = 314$ rad/s. The dc gain is equivalent to $R_mR_a/(R_m+R_a)$. The ac and dc gains had been plotted against the resistance (R_m) as shown in Fig. 4. The Figure shows that as R_m increases both the dc and ac gains of the filter increase. However, the increase of the dc gain saturates as R_m approaches 10 Ω. Furthermore, the ac gain attenuates the fundamental component of the main current by values from less than 0.5% to 2% while the dc gain attenuates the dc by values less than 20% to more than 80%. This shows how the proposed circuit makes the percentage of the dc component to the ac component increase from less than 2%, which is not measurable, to more than 15%. Taking into account the maximum input value for the amplifier, the tolerance in the passive filter components (L_{res} and C_{res}), and the amplifier offset value, the value of R_m can be chosen. In our design case, a value of 3 Ω has been applied.

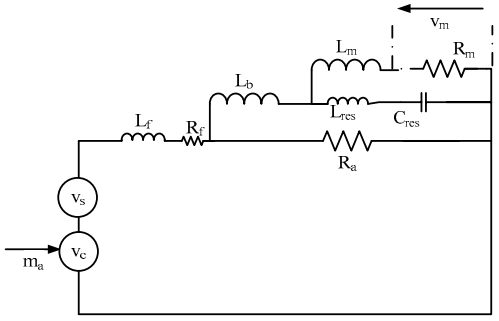

Fig. 6 A simplified circuit to the single phase inverter with the proposed measuring circuit

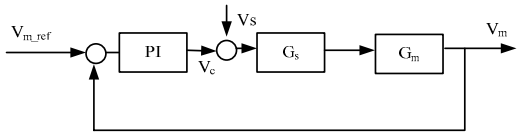

Fig. 7 Controller block diagram for the system equivalent circuit

To show how to design the resonance components values of L_{res} and C_{res}, a value of L_{res} was chosen with changing C_{res} in Equation (1). Fig. 5 shows the ac gain against the capacitor values with and without resonance circuit.

It is obvious that the minimum ac gain occurs in the resonance case, but because of the tolerance in the capacitor and inductor values, the capacitors are designed to be 20% more than the resonance value. The reason for this is to avoid the sharp increase in the ac gain less than the resonance value. The ac gain in the figure is attenuated to less than 25% in the designed point while the dc gain is not affected.

5. Controller Design

To simplify the system model, the causes of dc injection are collectively represented as a voltage source at the inverter output (v_s) as shown in Fig. 6.[11] Furthermore, the compensating voltage produced by off-setting the modulation index (m_a) of the inverter is considered a controllable dc voltage source (v_c). The inverter control will also respond to the residual fundamental ac component in v_m. However, the response is small compared to the normal inverter output voltage. The grid exhibits series inductance (L_f) and resistance (R_f).

The transfer function from the inverter output voltage to the current is simplified to a first order function:

$$G_s = \frac{K_s}{1+sT_s} \tag{3}$$

Where $K_s=1/R_f$, $T_s=L_f/R_f$. The transfer function of the measurement circuit was proposed before in Equation (1).

The block diagram of the closed-loop control system is shown in Fig. 7 where a PI controller is used to control the dc component of the current by off-setting the modulation index of the inverter. In the design of the controller, disturbance rejection and noise suppression were taken into account.[18]

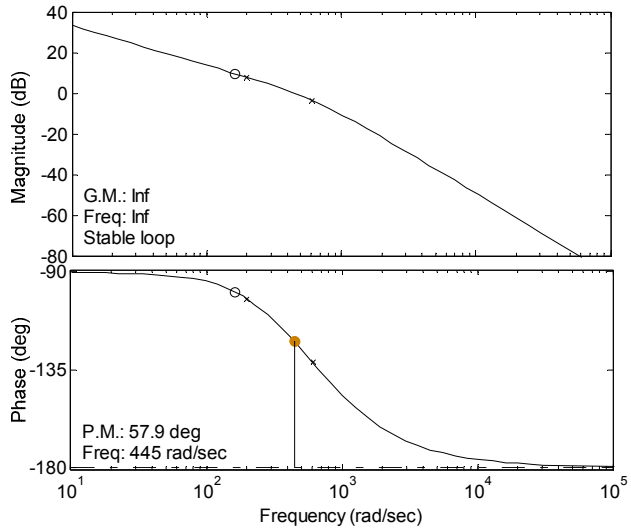

Fig. 8 Bode diagram shows controller design and system stability

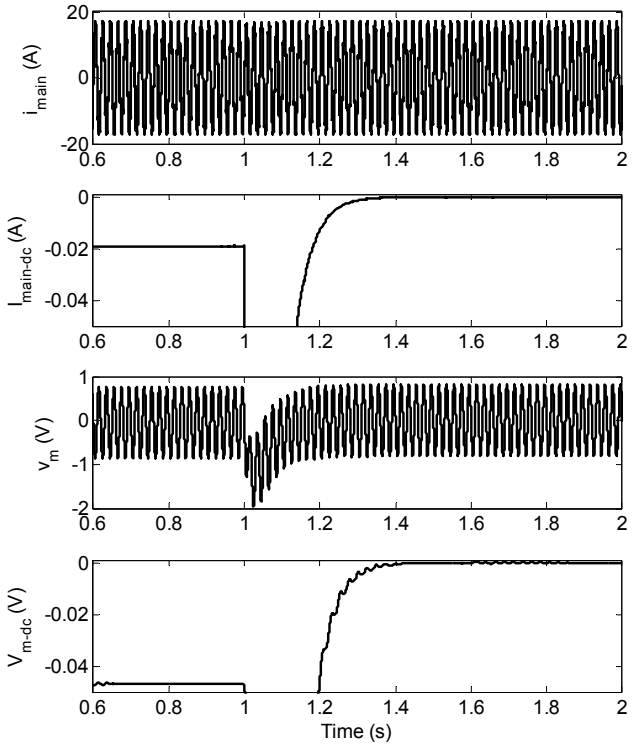

Fig. 9 Time-domain simulation results verifying dc component elimination

The Matlab control toolbox is used to design the PI controller. The bode plot of the system are shown in Fig. 8. The figure shows that the system is designed to show as fast response as possible without high peaks in the dc component.

6. Simulation Results

The time-domain simulation was carried out using Matlab/ Simulink for the system configuration as shown in Fig. 1. The dc link is a controlled voltage source emulating the renewable energy source supplying a single-phase grid-connected H-bridge inverter.

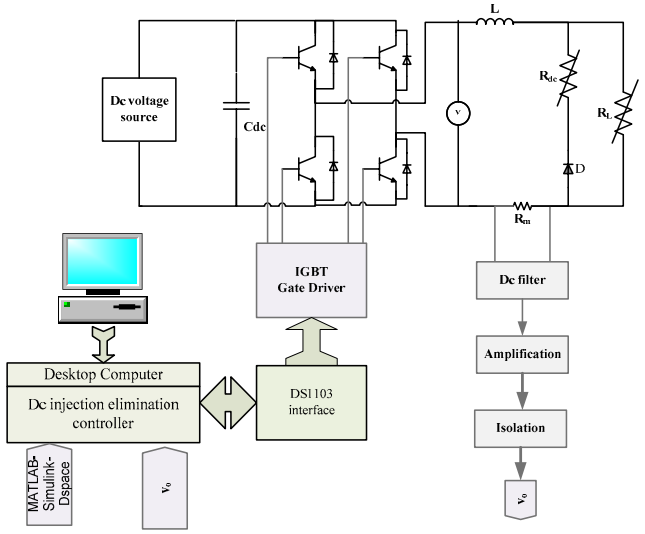

Fig. 10 The experimental test rig configuration

The dc link voltage is maintained to be constant at 400 V and the inverter is controlled to supply the grid with 2 kW power with unity power factor. Unequal on-state state voltages between the inverter arms are adjusted to produce a dc of 20 mA injected into the grid while the dc elimination controller is applied at t = 1 s from the start of the simulation. The simulation results are shown in Fig. 9, which illustrates the mains current (i_{main}), the mains dc component ($I_{main-DC}$), the filter output (v_m), and the dc component in the filter output voltage (V_{m-dc}).

The simulation results demonstrate that the dc can be eliminated by the controller and this proves the controller design based on a simplified method. Furthermore, the filter increases the signal-noise ratio of the dc component in v_m with respect to the residual ac component which is regarded as noise. The dc component in v_m becomes measurable after amplification. To demonstrate this, the dc component in the mains current is less than 0.2% while it is more than 5% in the output of the filter, corresponding to a 25 times improvement of the signal-noise ratio.

7. Experimental Verification

A block diagram of the experimental test rig setup is shown in Fig. 10 where a dc voltage source is connected to the H-bridge inverter, which supplies a passive load. To artificially cause a dc component in the inverter output current, a circuit of variable resistance connected to a diode is paralleled to the load resistance as shown in Fig. 10. The controller for the dc injection elimination and the inner loop for the inverter PWM process are programmed in Matlab/Simulink and implemented using an embedded dSPACE real time control system.[19]

The filter output is measured as shown in the figure and provided to the controller where the H-bridge inverter PWM control signals are generated. The dc injection elimination control is applied after 18 seconds from the start of the experiment.

The experimental results are shown in Figs. 11 and 12 where the data were collected on a digital scope and dSPACE respectively.

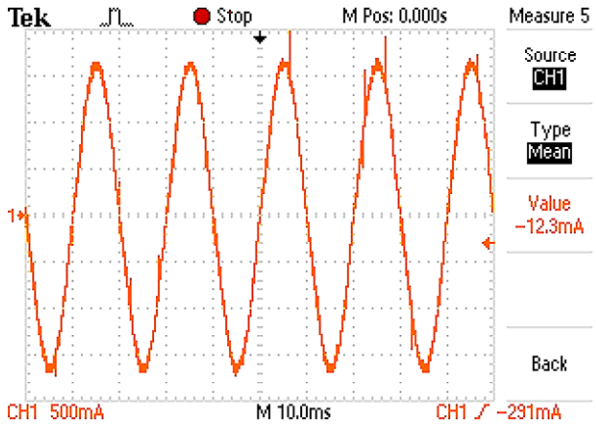

Fig. 11 Measured inverter output current (i_{main})

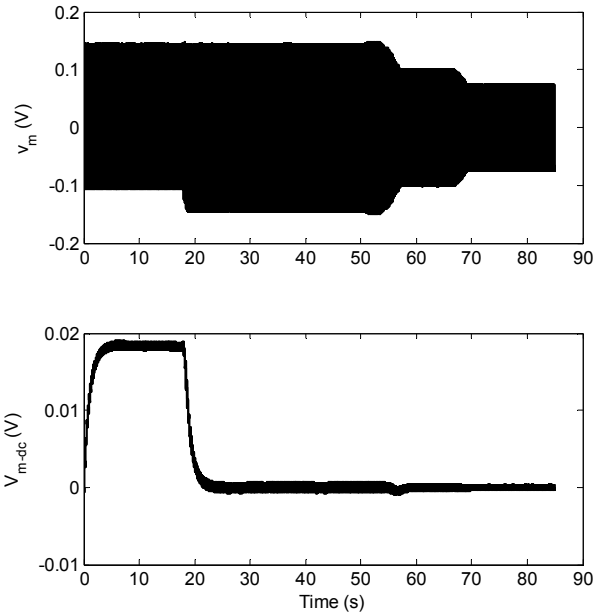

Fig. 12 Experimental results verify dc elimination

Fig. 11 shows the inverter output current before dc component elimination, which contains a dc component. Fig. 12 shows the output voltage of the measuring filter circuit v_m. The variable resistance was adjusted to produce almost 12.3 mA dc component in the inverter output current whose fundamental ac component is approximately 1.06 A, as shown in Fig. 11.

It is clearly shown in Fig. 12 that the controller eliminates the dc component to a non-significant level. Furthermore, the test results show that as the inverter output current changes, the controller keeps the dc-injected current at the same level, which remains to be insignificant. This is particularly useful in renewable energy systems where the input power is always fluctuating.

The experimental results show a slight divergence from the expected ideal characteristics and this is due to the tolerance of the passive filter component values. With this, the filter can still adequately sense the dc component in the inverter output current. As a demonstration, the dc component is only 0.8% in the inverter output current while it is almost 13% in the filter output voltage signal. Consequently, the objective of the research has been achieved.

8. Conclusion

Dc injection is of growing concern due to the increasing usage of single-phase inverters as the demand for small scale renewable power generation increases. One of the challenges to eliminate the dc injection is to accurately measure the small dc component contained in the inverter output current. This is particularly difficult as the fundamental ac current component is relatively large.

In this paper, a method to eliminate the dc injection of a single-phase H-bridge inverter is proposed. The proposed method is based on designing a passive filter to make the dc component more measurable in the filter output. A simplified method to design the compensating control was proposed for the inverter PWM process.

The method has been verified by both simulation and experimental test. The simulation and experimental results demonstrate that the proposed method improves the accuracy of measuring of the very small dc component. This improvement helps removing the dc component to meet the obligatory local and international standards.

REFERENCES

1. Bae, K. and Shim, J. H., "Economic and environmental analysis of a wind-hybrid power system with desalination in Hong-do, South Korea," Int. J. Precis. Eng. Manuf., Vol. 13, No. 4, pp. 623-630, 2012.
2. Choi, K.-S., Yang, D.-S., Park, S.-Y., and Cho, B.-H., "Design and performance test of hydraulic PTO for wave energy converter," Int. J. Precis. Eng. Manuf., Vol. 13, No. 5, pp. 795-801, 2012.
3. Alsayegh, O., Alhajraf, S., and Albusairi, H., "Grid-Connected renewable energy source systems: Challenges and proposed management schemes," Energy Conversion and Management, Vol. 51, No. 8, pp. 1690-1693, 2010.
4. Carrasco, J. M., Franquelo, L. G., and Alfonso, N. M., "Power-Electronic systems for the grid integration of renewable energy sources: A survey," IEEE Transactions on Industrial Electronics, Vol. 53, No. 4, pp. 1002-1016, 2006.
5. Kjaer, S. B., Pedersen, J. K., and Blaabjerg, F., "A review of Single-Phase Grid-Connected inverters for photovoltaic modules," IEEE Transactions on Industry Applications, Vol. 41, No. 5, pp. 1292-1306, 2005.
6. Kjaer, S., Pedersen, J., and Blaabjerg, F., "A review of Single-Phase Grid-Connected inverters for photovoltaic modules," IEEE Transactions on Industry Applications, Vol. 41, No. 5, pp. 1292-1306, 2005.
7. González, R., Gubía, E., López, J., and Marroyo, L., "Transformerless Single-Phase Multilevel-Based Photovoltaic Inverter," IEEE Transactions on Industrial Electronics, Vol. 55, No. 7, pp. 2694-2702, 2008.
8. Salas, V., Olías, E., Alonso, M., and Chenlo, F., "Overview of the

legislation of DC injection in the network for low voltage small Grid-Connected PV systems in spain and other countries," Renewable and Sustainable Energy Reviews, Vol. 12, No. 2, pp. 575-583, 2008.

9. Haeberlin, H., "Evolution of inverters for grid connected PV-Systems from 1989 to 2000," 17th EUR Photovoltaic Solar Energy Conference, 2001.
10. Armstrong, M. and Jacmj, D., "Auto-Calibrating DC Link Current Sensing Technique for Transformerless, grid Connected, H-Bridge inverter systems," IEEE Transactions on Power Electronics, Vol. 21, No. 5, pp. 1385-1393, 2006.
11. Salas, V., Alonso, M. A., Olíasa, E., Chenlob, F., and Barrado, A., "DC current injection into the network from PV inverters," Solar Energy Materials and Solar Cells, Vol. 91, No. 9, pp. 801-806, 2006.
12. Noguchi, S. T., "A new Three-Level Current-Source PWM inverter and its application for grid connected power conditioner," Energy Conversion and Management, Vol. 51, No. 7, pp. 1491-1499, 2010.
13. Gonzalez, R., Lopez, J., Sanchis, P., and Marroyo, L., "Transformerless inverter for Single-Phase photovoltaic systems," IEEE Transactions on Power Electronics, Vol. 22, No. 2, pp. 693-697, 2007.
14. Kerekes, T., Teodorescu, R., Rodríguez, P., Vázquez, G., and Aldabas, E., "A new High-Efficiency Single-Phase transformerless PV inverter topology," IEEE Transactions on Industrial Electronics, Vol. 58, No. 1, pp. 184-191, 2011.
15. Salas, V., Olias, E., Alonso, M., Chenlo, F., and Barrado, A., "Dc current injection into the network from PV grid inverters," IEEE 4th World Conference on Photovoltaic Energy Conversion, Vol. 2, pp. 2371-2374, 2006.
16. Dahidah, M. and Agelidis, V., "Single-Carrier sinusoidal PWM-Equivalent selective harmonic elimination for a Five-Level voltage source converter," Electric Power Systems Research, Vol. 78, No. 11, pp. 1826-1836, 2008.
17. Lee, Y.-J. and Lee, S.-K., "Classification of noise sources in a printer and its application to the development of sound quality evaluation," Int. J. Precis. Eng. Manuf., Vol. 13, No. 4, pp. 491-499, 2012.
18. Levine, W., "The control handbook," CRC Press, 2006.
19. dSPACE, "DS1103 PPC controller board," http://www.dspaceinc.com/ww/en/inc/home/products/hw/singbord/ppcconbo.cfm, (Accessed 1 June 2010).